2009 IEEE Industry Applications Society Annual Meeting

4-8 October 2009 Houston, Texas, USA

IEEE
Celebrating 125 Years of Engineering the Future

IAS
IEEE INDUSTRY APPLICATIONS SOCIETY

Papers by Session

Appliance Technologies and Systems

- Quality Assurance Testing for Magnetization Quality Assessment of BLDC Motors used in Compressors
  Kwangwoon Lee, Jongman Hong, Sang Bin Lee and Sangtaek Lee
- Estimation of Magnet Reduction in Single-Phase Line-Start Permanent Magnet Synchronous Motor
  Liang Fang, B. H. Lee, Jung-Pyo Hong and Hyuk Nam
- Inductance Measurement of Interior Permanent Magnet Synchronous Motor in Stationary Reference Frame
  Tao Sun, Soon-O Kwon, Jung-Pyo Hong and Geun-Ho Lee

Click on title for a paper.

Estimation of Magnet Reduction in Single-Phase Line-Start Permanent Magnet Synchronous Motor

Liang Fang, B. H. Lee
Student Member, IEEE
HanyangUniversity
17 Haengdang-dong, Seongdong-gu
Seoul 133-791, Korea
fangliangicw@hotmail.com

Jung-Pyo Hong
Senior Member, IEEE
HanyangUniversity
17 Haengdang-dong, Seongdong-gu
Seoul 133-791, Korea
hongjp@hanyang.ac.kr

Hyuk Nam
LG Electronics Inc.
Changwon 641-711, Korea
hnam@lge.com

***Abstract* -- This paper describes an efficient approach for skillfully guiding the magnet reduction design in a single-phase line-start permanent magnet motor(LSPMM) without worsening motor torque and efficiency performances. The relevant decrease of magnet torque due to magnet reduction is compensated by improving the unique hybrid torque characteristic, that enhancing the balance ratio of reluctance torque to magnet torque. The increased reluctance toque also benefits to motor efficiency performance. Based on an existing LSPMM model, a simulation method, "torque-efficiency map" is proposed to estimate proper reduction of magnet according to assumed saliency ratio. Then, with estimated reduced amount of magnet, a flexible double-layer interior-PM(IPM) rotor structure is optimized with given torque and efficiency constrains. In this paper, the finite element analysis(FEA) combined with equivalent circuit method is used to calculate the LSPMM characteristics and performances. The validity of estimation of magnet reduction based on torque-efficiency map is verified by testing LSPMMs with reduced magnet usage.**

***Index Terms*-- Double-layer IPM design, FEA, hybrid torque, LSPMM, magnet reduction design, torque-efficiency map.**

I. INTRODUCTION

The single-phase line-start permanent magnet motor (LSPMM) has beneficial attributes of induction motor(IM) and interior permanent magnet synchronous motor(IPMSM), that it has self-starting ability with fed directly from commercial voltage source without any power electronic devices, and it guarantees high efficiency performances at steady state synchronous operation[1],[2]. Therefore, from the energy saving standpoint, the LSPMM substituting LSIM are widely used in household applications, such as compressors of air-condition and refrigerator, which has largest portion of power used[2],[3].

By utilizing the unique hybrid torque generation from the IPM rotor, the torque and efficiency performance of LSPMM are improved with PM buried in the cage-bar rotor core. In addition, the cage bar losses minimization, and unit-power-factor are realized at steady state operation[2],[4].

On the other hand, the buried PM make braking torque, that weaken the asynchronous starting torque by means of cage bars in start-up operation[5]. Therefore, the magnet usage buried in LSPMM rotor should be judged properly to guarantee enough starting torque, as well as to improve synchronous torque and motor efficiency performances.

In this paper, a double-layer IPM design is employed to an initial LSIM. It is a popular design approach that by utilizing the IPM rotor structure advantage to improve machine performance. However, the high cost of PM materials always limited its application. Therefore, an effective approach for guiding the reduction of magnet usage in PM machines design is really expected, but there are no papers focused on it. In this paper, an approximate method is proposed for estimating the magnet reduction in the LSPMM design with given torque and efficiency constrains, thus named as "torque-efficiency" map. Its availability is verified by estimating the magnet reduction design in LSPMM.

The main characteristics of LSPMM, such as back electromotive force(back-EMF), and inductance(L), are quite sensitive to the rotor inner structure, including PM segments, buried air-gap regions and cage bars. In particular, the adopted double-layer IPM rotor design is a different and time-consuming work. Therefore, a widely recognized optimization technique, response surface methodology(RSM) is applied to the LSPMM optimal design for satisfying the predicted machine characteristics by torque-efficiency map corresponding to magnet usage reduction.

For analyzing the torque and efficiency performances of LSPMM, equivalent circuits method(ECM) is performed, and 2-dimensional(2-D) finite element analysis(FEA) is applied to calculate machine characteristics, such as back-EMF and *d-q* axis inductances. In final, the machine torque and efficiency performances are measured by experiment method. And, a good agreement well confirmed the present LSPMM performance analysis by ECM.

II. MODELS AND METHOD

A. LSIM and LSPMM

In this paper, an existing 2000W, 220V/50Hz single-phase LSIM used as compressor in air-condition is introduced as base model. It has 28 stator slots and 34 cage bars. Fig. 1 shows its cross section and stator main/auxiliary winding connection circuit. And, a prototype LSPMM with double-layer IPM rotor is designed and fabricated based on the LSIM for 3 [%] efficiency improvement, as Fig. 2 illustrates. TABLE I compares their tested performances, that stating

torque, maximum torque and efficiency are emphasized.

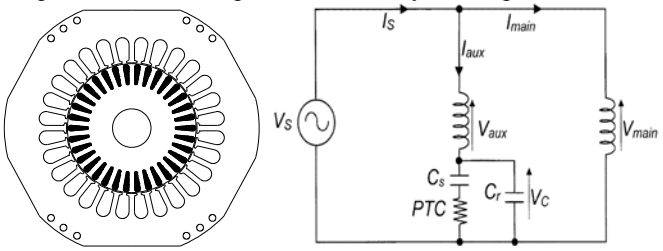

Fig. 1 Cross section of LSIM and single-phase windings connection circuit

TABLE I
TEST PERFORMANCES OF LSIM AND PROTOTYPE LSPMM

Items	Unit	LSIM_Base	LSPMM_"P_o"	Improve
Output Power	[W]	2000	2000	-
Start Torque	[Nm]	2.10	2.9	+38 [%]
Max. Torque	[Nm]	13.3	13.2	-
Ave. Torque	[Nm]	6.65	6.64	-
Efficiency	[%]	84.7	87.9	+3.2[%]
Power factor	[%]	98.5	99.5	+0.6[%]

B. LSPMM Characteristic Analysis

In this paper, single-phase LSPMM is examined focusing on asynchronous starting torque, maximum torque, and high efficiency performance at steady states. A well recognized equivalent circuit method is performed for simply analysis.

1). *Asynchronous Starting Torque Analysis.*

During asynchronous start-up operation, the starting torque (*T_st*) of the LSPMM is mainly considered by the average cage torque(*T_cage*) minus the magnet braking torque (*T_mag*), as Fig. 3(a) illustrates[5]. *T_cage* is developed by cage-bars rotor of LSIM, and the *T_mag* is produced due to the reaction of currents induced from the magnet flux in stator windings[5]. In practice, the enough asynchronous *T_st* must be generated for starting the LSPMM successfully. Fig. 3(b) shows the variation of feeding currents in each of main/auxiliary windings corresponding to the asynchronous *T_st* generation. Also, from the Fig. 1 shown stator electric circuit, the starting capacitances [C_s], running capacitances [C_r] and positive temperature coefficient(PTC) are connected to auxiliary winding in parallel for increasing the starting torque and power factor[6]. By performing the equivalent circuit proposed by T.J.E. Miller[5], the starting torque performance is examined with the variation of main/auxiliary windings ratio, cross section of care bars, and assistant capacitors C_s and C_r, as Fig. 4 shows. The proper values for LSPMM design are chosen as "red lines" shows.

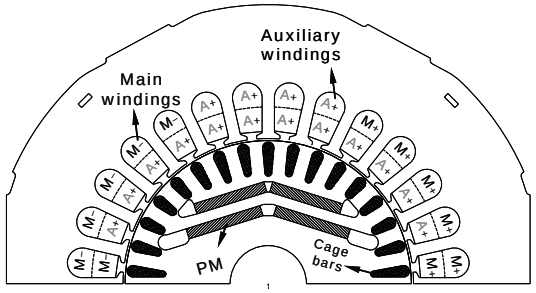

Fig. 2 Single-phase LSPMM model with double-layer IPM rotor design

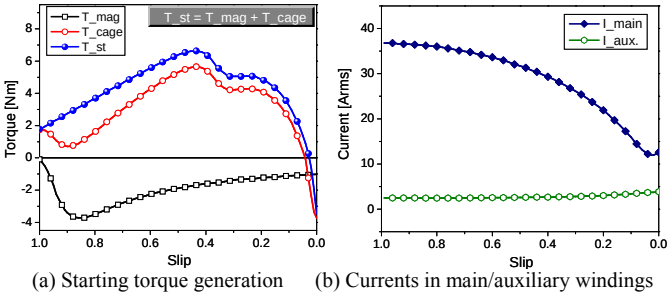

(a) Starting torque generation (b) Currents in main/auxiliary windings

Fig. 3 LSPMM start-up performance simulation by ECM

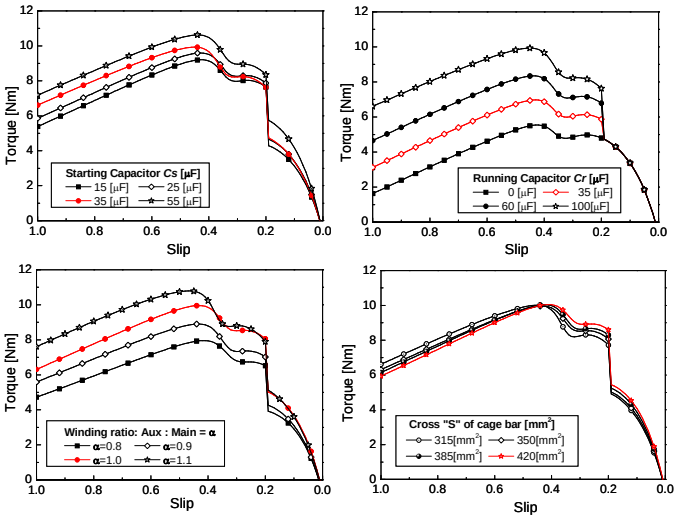

Fig. 4 LSPMM asynchronous starting torque examined by ECM

2). *Steady State Performance Analysis*

The LSPMM performances at steady state operation are analyzed by introducing a developed equivalent circuit[6]. In theory, the single-phase LSPMM is converted into a two-phase frame of *d-q* plane, and then the unbalanced field is dealt with symmetrical coordinate method[7]. Fig. 5 shows the vector diagram in *d-q* plane. The torque and efficiency performances are calculated by carrying out equivalent circuit, that composed of *d*-axis/*q*-axis positive sequence circuit and negative sequence circuit respectively, as Fig. 6 gives. The required simulation parameters in ECM, such as fundamental component of phase back-EMF, *d-q* axis inductances varying with currents and current phase angles, and iron loss are precisely calculated by 2D FEA.

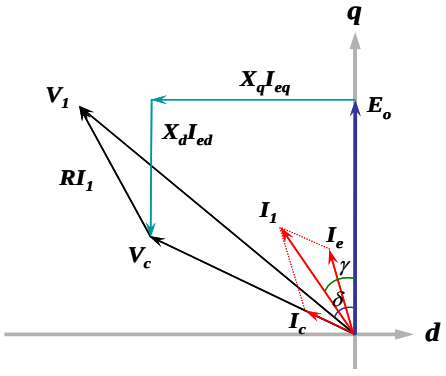

Fig. 5 Vector diagram of the single-phase LSPMM

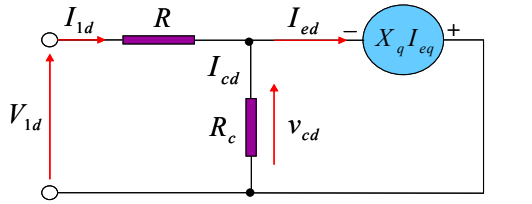

(a) *d*-axis of positive sequence

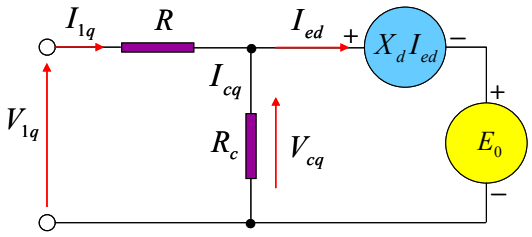

(b) *q*-axis of positive sequence

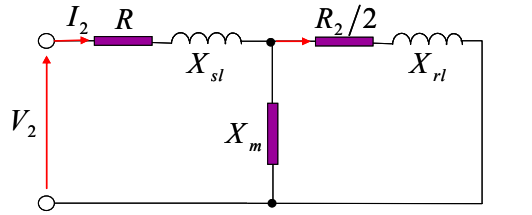

(c) Negative sequence

Fig. 6 Equivalent circuits of single-phase LSPMM

The steady state performances of single-phase LSPMM are similar to IPMSM, of that generates hybrid synchronous torque. According to the presented vector diagram and *d-q* axis equivalent circuit, as well as the stator electric circuit, the voltage and current equations, and output power, hybrid torque production, motor efficiency performance calculations are obtained as following equations[8]:

$$\begin{cases} I_{1d} = I_{ed} + I_{cd} \\ I_{1q} = I_{ed} + I_{cq} \end{cases} \quad [1]$$

$$\begin{cases} V_{1d} = RI_{1d} - X_q I_{eq} \\ V_{1q} = RI_{1q} + X_d I_{ed} + E_o \end{cases} \quad [2]$$

$$\begin{cases} \mathrm{I_{aux}} = \dfrac{1}{\sqrt{2}}\left[\mathrm{I_1}\left(1 + j\dfrac{\cot\varepsilon}{\beta}\right) + \mathrm{I_2}\left(1 - j\dfrac{\cot\varepsilon}{\beta}\right)\right] \\ \mathrm{I_{main}} = -\dfrac{1}{\sqrt{2}\beta}\csc\varepsilon\left[\mathrm{I_1} - \mathrm{I_2}\right] \end{cases} \quad [3]$$

$$\begin{cases} P_{out} = P_1 + P_2 = \left(\mathrm{Re}(\mathrm{V_1 I_1^*}) - R\mathrm{I_1^2}\right) - \left(\mathrm{Re}(\mathrm{V_2 I_2^*}) - R\mathrm{I_2^2}\right) \\ \eta_{eff} = \dfrac{\mathrm{V_S \cdot I_S}}{P_{out}} \times 100\% \end{cases} \quad [4]$$

$$\begin{cases} T_{Hy} = T_{Ps} + T_{Ns} = P_1/\omega_s + P_2/\omega_s \\ {*T_{Ps}} = \left(T_M + T_R\right) = p\left(E_o I_{1q} + (L_d - L_q) I_{1d} I_{1q}\right) \end{cases} \quad [5]$$

where, I_e is effective current in the positive sequence circuit, I_c is current consumed in iron loss, R_a is equivalent phase winding resistance, R_c is equivalent iron loss resistance, β is effective turn ratio between the main/auxiliary windings, ε is electrical angle between *d-q* axis, E_o is no-load back-EMF.

III. Magnet Reduction and Double-layer IPM Rotor

The LSPMM is synchronous hybrid PM/reluctance brushless motor[4]. At synchronous operation, the hybrid torque generation can be mainly represented by the above torque equation (5). In this paper, the magnet reduction design in LSPMM is realized by emphasizing the hybrid torque characteristic, that help to lower the dependency on magnet, and improve torque and efficiency performance.

A. Hybrid Torque Analysis

From the hybrid torque generation characteristic, the identical maximum hybrid torque(T_{Hy}) can be generated with different balance ratio of reluctance torque(T_R) to magnet torque(T_M), such as (3:10) and (6:7), as Fig. 7 (a), (b) show.

It is well known that the high rotor saliency benefits to reluctance torque T_R production, and the less magnet usage results in the decrease of magnet torque T_M production. Therefore, in the magnet reduction design in LSPMM, the geometry of IPM rotor structure is optimized for achieving high rotor saliency, so that the reluctance torque is improved to compensate the magnet torque T_M component.

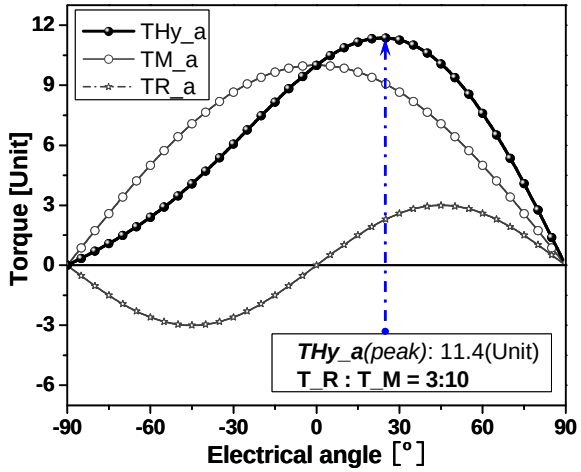

(a) Indentify hybrid torque $T_{\_peak}$ with low ratio of ($T_{\_R}$ / $T_{\_M}$)

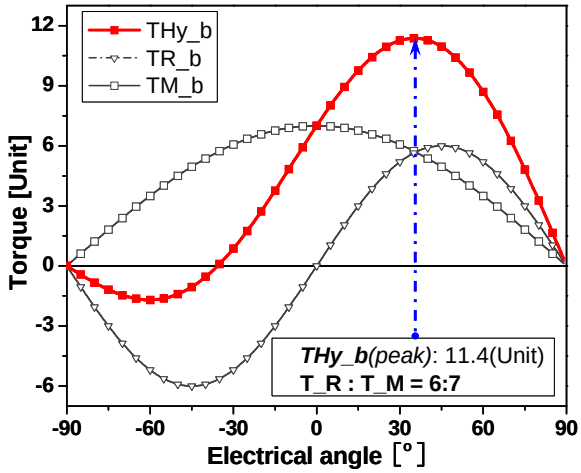

(b) Indentify hybrid torque $T_{\_peak}$ with high ratio of ($T_{\_R}/T_{\_M}$)

Fig. 7 Hybrid torque characteristics analysis for magnet reduction design

B. *Torque-Efficiency Map Analysis*

In the magnet reduction design, the LSPMM performance of torque and efficiency are constrained as the prototype LSPMM achieved, that maximum output $T\_max.$=13.0[Nm] and efficiency at steady state η=90[%] by equivalent circuit method. Although the calculated results show difference with their tested values, ($T\_max.$=13.2[Nm] and η=87.9[%] as TABLE I lists), the calculated torque and efficiency constrains are still used as a standard in LSPMM characteristics analysis.

An efficient method, "torque-efficiency map" is proposed for directly judging whether the LSPMM design can satisfy the both constrains at the same time, and also estimating the possible reduction of magnet, according to the motor basic characteristics, phase back-EMF and *d*-*q* axis inductances, which can be quickly and precisely calculated by 2D FEA.

By carrying out the equivalent circuits presented in the Section II-(2), the torque and efficiency characteristics can be predicted as functions of phase back-EMF(E_o) and *d*-axis(or *q*-axis) inductance *Ld*(or *Lq*). Further, with reasonable variation ranges of E_o and *Ld*[or *Lq*], the torque and efficiency distributions can be mapped, as Fig. 8 illustrates. The inductances *Ld* and *Lq* can be related by defining rotor saliency ratio as [γ=*Lq*/*Ld*] for simplicity. Based on the prototype LSPMM characteristics, the torque-efficiency map with [γ=2.5]. The superposition region is obviously satisfies the torque and efficiency constrains, that enclosed by the red and blue heavy lines, which are respectively considered as the constrain boundaries of maximum torque 13.0[Nm] and efficiency 90[%] in the LSPMM design.

It is found that the improvement of torque and efficiency along different design directions, that the larger E_o helps to increase $T\_max.$, but against to efficiency improvement, and the lower *d*-axis inductance benefits to both torque and efficiency. The corresponding point "P_o" appears in the enclosed region confirmed the prototype LSPMM satisfied the torque and efficiency constrains.

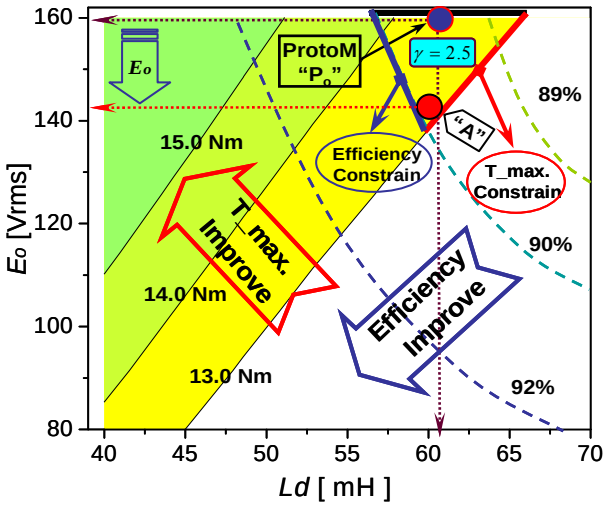

Fig. 8 Torque-Efficiency map based on prototype LSPMM

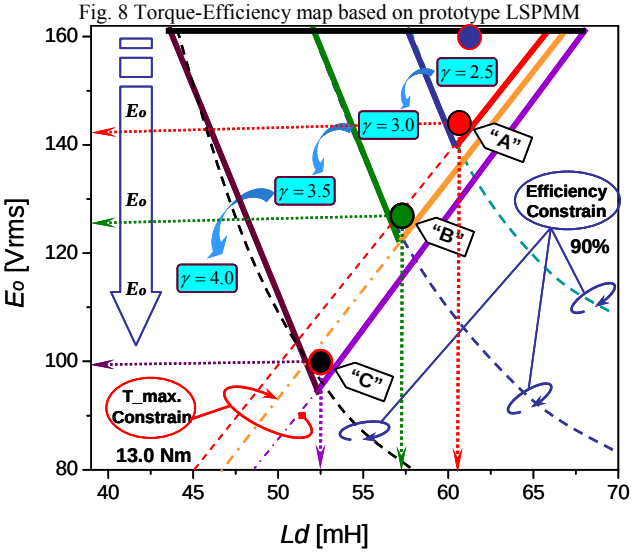

Fig. 9 Torque-Efficiency map for estimating magnet reduction

In the torque-efficiency map analysis, the magnitude of E_o is generally through to be proportional to magnet usage. Therefore, the decreased of E_o can be used to estimate the reduction of magnet used for guarding the LSPMM redesign. Therefore, the point "P_o" in the enclosed region indicates that the prototype LSPMM is not the optimum design from the minimum magnet standpoint, since "P_o" corresponding to a higher E_o value [160(V_{rms})] in the design region. A developed design, marked as "A", corresponding to lower E_o value [142(V_{rms})] and similar *d*-axis inductance [62(mH)], but just satisfying the torque and efficiency constrains. It is thought to be the desired design point for saving magnet material. Due to the approximate 10% decreasing of E_o, about 10% amount of magnet usage in LSPMM is estimated to be reduce by redesign "P_o" to "A".

By developing this torque-efficiency map method, the design regions with higher saliency ratio γ {3.0; 3.5; 4.0} can be determined effectively. As the Fig. 9 shows, the higher saliency ratio γ will enlarge the enclosed superposition region of the torque and efficiency constrains, and more reduction of

magnet usage can be expected.

Similar to design point "A" analysis, the magnet minimum design point can be decided in each region, and the magnet reduction is estimated by comparing to the prototype LSPMM "P_o", that corresponds to back-EMF and *Ld* [160(V_{rms}), 61.5(mH)] in map of {γ=2.5}, as Fig. 9 shows. Correspondingly, the design point "B", corresponding to about [120(V_{rms}), 55.0(mH)] in region of {γ=3.0}, by which 25% magnet reduction is estimated. Also the design point "C", corresponding to nearly [105(V_{rms}), 52.0(mH)] in region of {γ=3.5}, and 35% magnet reduction is estimated. In conclude, higher rotor saliency benefits to magnet reduction in LSPMM with given torque and efficiency constrains.

The next work of LSPMM design is to achieve these predicted characteristic, that phase back-EMF and *d-q* axis inductances with required rotor saliency by using the corresponding estimated reduction of magnet material.

C. Double-layer IPM Rotor Design

The LSPMM rotor configuration, including PM segments and buried air-gap fields, are optimized with given torque and efficiency constrains for realizing magnet reduction.

Base on the prototype LSPMM model, the IPM rotor is rebuilt with less amount of magnet as estimated. The design variables of double-layer IPM rotor structure, and the design limits for mechanical strength consideration, are illustrated in Fig. 10. The reduced dimension of magnet segments is visualized in Fig. 11. The identical length of each PM segments [$L_{\_PM}$] is assumed, and the slope angle of side PM segment [α] combining with the distance between PM segments [G_o] are optimized for achieving the objective of phase back-EMF and *d-q* axis inductance, predicted by the torque-efficiency map analysis. In particular, the buried air-gap regions are enlarged in design for decreasing the *d*-axis inductance, that benefits to improve the rotor saliency, and increase reluctance torque generation.

The adopted double-layer IPM rotor structure is efficiently optimized with the help of response surface methodology[10]. The design objective functions are chosen as the phase back-EMF, and *d-q* axis inductances, for verifying the effectiveness of predicted results by torque-efficiency map.

The amount of PM used in prototype LSPMM "P_o" model is standard as 100[%], and the optimal design "A" model with 90[%] PM, and design "B" model with 75[%] PM, are illustrated with the determined design variables in Fig. 12. Both of the LSPMM "A" and "B" models achieved almost same torque and efficiency with prototype LSPMM "P_o" model. But, the design model "C" with 65[%] PM can not satisfy constrains successfully by optimizing the double-layer IPM rotor structure. TABLE II lists the characteristics comparison of each model in the magnet reduction design.

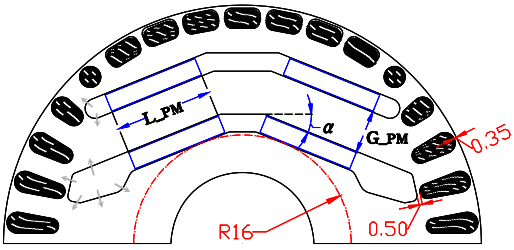

Fig. 10 Base model and design variables of double-layer IPM rotor

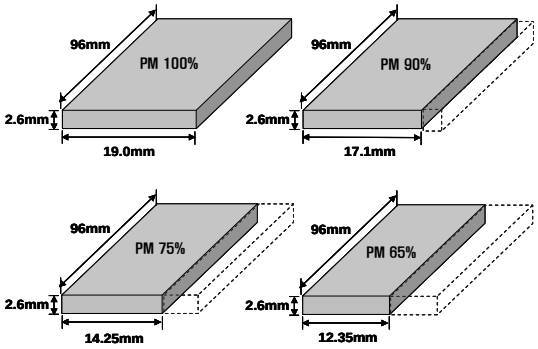

Fig. 11 Dimensions of reduced magnet in double-layer IPM design

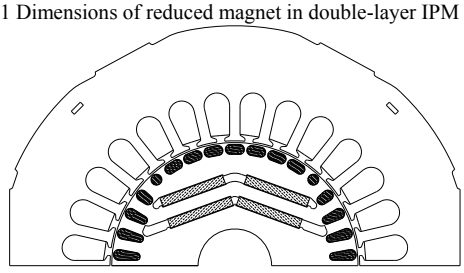
(a) Prototype LSPMM "P_o"[100% PM]: (α=20°, G_PM=3.9mm)

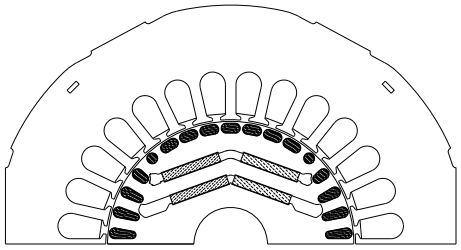
(b) Optimal LSPMM "A" [90% PM]: (α=20°, G_PM=4.3mm)

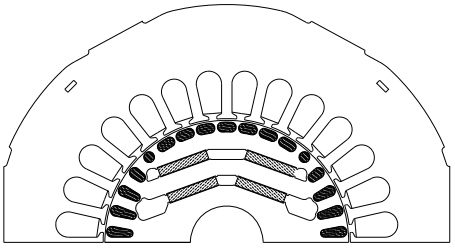
(b) Optimal LSPMM "B" [75% PM]: (α=20°, G_PM=5.4mm)

Fig. 12 Magnet reduction design of double-layer IPM rotor LSPMM models

TABLE II
PERFORMANCE COMPARSION IN MAGNET RESDUCTION (ECM)

Model	IM	M_"P_o"	M_"A"	M_"B"	M_"C"
PM use [%]	0	100	90	75	65
BEMF[V_{rms}]	0	160	141.3	123.1	101.5

Model	IM	M_"P_o"	M_"A"	M_"B"	M_"C"
PM use [%]	0	100	90	75	65
Saliency	0	2.5	2.5	3.0	3.2
T_Max.[Nm]	13.2	13.2	13.0	13.0	12.5
T_Ave.[Nm]	6.5	6.5	6.5	6.5	6.5
Efficiency[%]	88.0	90.8	91.0	91.0	90.0

D. *Limit of Rotor Saliency Improvement*

The rotor saliency is created, since the high reluctance exists along *d*-axis due to the low permeability of buried PM and air-gap regions, while along *q*-axis between magnet poles, existing no magnetic barriers, the reluctivity to magnetic flux is very low[2],[9]. As the rotor saliency definition in term of *d*-*q* axis inductances, the rotor saliency can be enhanced by enlarging the difference of *d*-axis and *q*-axis inductances. But, the decrease of *d*-axis inductance is different without increasing the magnet usage, even the buried air-gap regions can be utilized at a certain extend. Also, the increase of *q*-axis inductance is also quite finite due to the flux-barriers and saturation effect[2]. As the design "C" model with 65 [%] PM need saliency {γ=3.5} to satisfy the torque and efficiency constrains, but just {γ=3.2} can be achieved by optimizing double-layer IPM rotor geometry. The saliency {γ=3.5} can be achieved by adopting three-layer IPM design, but will cause low mechanical robustness and high manufacture cost.

IV. Results And Discusses

A. *Torque Performance Test*

The starting torque performance and maximum output torque operation of the basic LSIM and fabricated LSPMM "B" are tested and compared, as Fig. 13 and Fig. 14 show respectively. The LSPMM "B" generates higher starting torque than the prototype LSPMM "P_o" (TABLE I lists), about 140[%] larger than that of LSIM. And the maximum output torque at steady state is tested as 13.2[Nm] contract to the 13.0[Nm] calculated by the presented ECM. It is a little lower than LSIM test result 13.3[Nm], but satisfying torque constrain of LSPMM design.

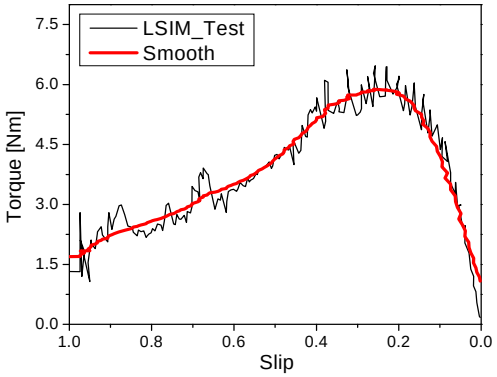

(a) Starting torque of LSIM by test

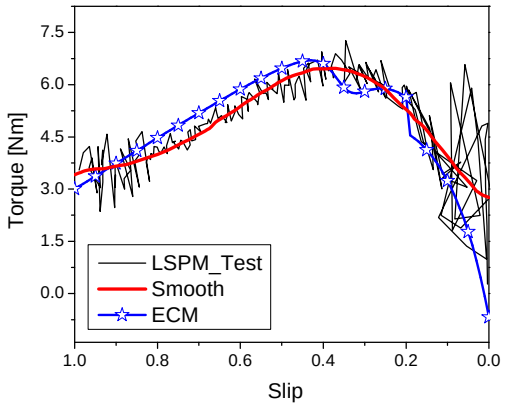

(b) Starting torque of LSPMM "B" by test and ECM

Fig. 13 Asynchronous starting torque results comparison

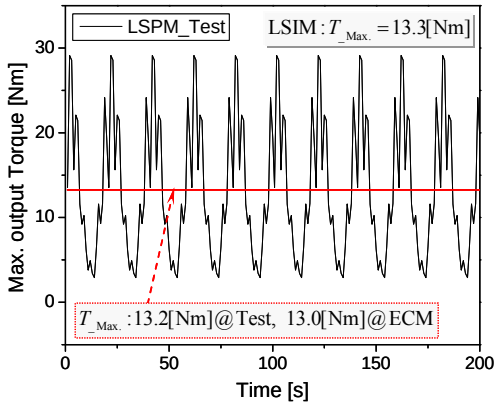

Fig. 14 Maximum output torque at synchronous operation

B. *Efficiency Performances Test*

According to the equivalent circuit analysis, the optimized LSPMM "B" achieved efficiency 90[%] similar to LSPMM "P_o" at steady state operation, but realized 25[%] reduction of magnet usage. On the other hand, the efficiency of prototype double-layer design LSPMM "P_o" improved 3[%] to the base LSIM, that is verified by test results, as TABLE I given.

Therefore, the LSPMM "B" is fabricated and its on-load performances are tested (temperature is maintained at 25°C by fan-cooling), as Fig. 15 illustrates. Then, its efficiency is compared with LSIM also, as Fig. 16 gives. Although the calculated results by using ECM are higher than their corresponding tested results, the 3[%] improvement of efficiency is still proved, since the almost same proportional enlarged between the calculated result and test data. The tested main performances of the above three motors are compared, as Fig. 17 shows, the proper magnet reduction design without worsening machine performance is confirmed.

(a) LSPMM "B" stator and rotor configuration

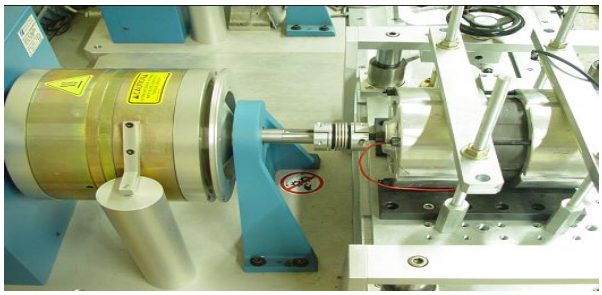

(b) Testing apparatus for machine performance measurement

Fig. 15 Fabricated LSPMM and experiment apparatus for torque and efficiency measurement

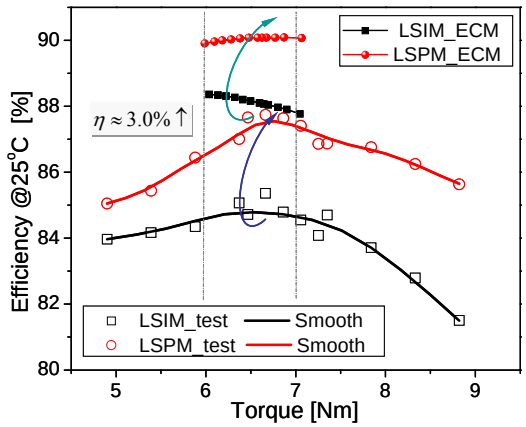

Fig. 16 Efficiency performance comparison (Test temperature 25ºC)

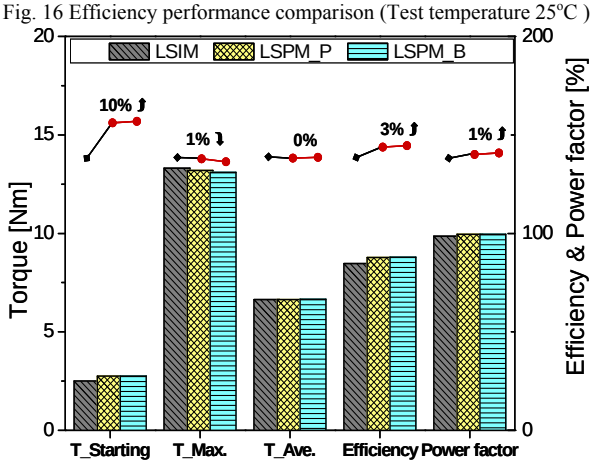

Fig. 17 Main performnaces comparison between LSIM and LSPMMs

CONCLUSION

This paper has presented a theoretical and experimental study of magnet reduction in a single-phase LSPMM by emphasizing double-layer IPM structure advantage without worsening main machine performances. The validity of proposed "torque-efficiency map", for estimating possible reduction of magnet with condition of rotor saliency improvement is verified to be effective through the LSPMM optimal design with estimated less magnet usage, and the given constrains of torque and efficiency are satisfied. The test results of LSPMM at both asynchronous start-up operation and steady state performance well validated the presented analysis approach by equivalent circuit method coupled with 2D FEA.

On the other hand, to improve the rotor saliency with reduce magnet is quite different and limited by the rotor structure. Much more complicate rotor structure may realize further magnet reduction, but results in unavoidable increasing of manufacture cost.

REFERENCES

[1] Timothy J. E. Miller, "Single-Phase Permanent-Magnet Motor Analysis", *IEEE Trans. On Indus. Appl., Vol. IA-21, No. 4, May/June 1985.*

[2] Nicole Bianchi, Thomas M. Jahns, "Design, Analysis, and Control of Interior PM synchronous Machines", *IEEE-IAS* Electrical Machines Committee.

[3] John M. Miller, *Propulsion systems for hybrid vehicles*, The Institution of Electrical Engineers, 2004. pp. 168-170

[4] Timothy J. E. Miller, "Line-start Permanent-Magnet Single-phase Steady-State Performance Analysis", *IEEE Trans. On Indus. Appl., Vol.40. No. 2, March/April 2004.*

[5] Mircea Popescu, Timothy J. E. Miller, Malcolm McGilp, Giovanni Strappazzon, Nicolla Trivillin, Roberto Santarossa, "Asynchronous Performance Analysis of a Single-Phase Capacitor-Start, Capacitor-Run Permanent Magnet Motor", *IEEE Trans. On Energy Conversion., Vol.20. No. 1, March 2005.*

[6] G. H. Kang, B.K. Lee, H. Nam, J. Hur, and J. P. Hong, "Analysis of Single-Phase Line-Start Permanent-Magnet Motors Considering Iron Loss and Parameter Variation With Load Angle," *IEEE Trans. On Indus. Appl., Vol. 40, No. 3, May/June 2004.*

[7] Jie Zhou, and King-Jet Tseng, "Performance Analysis of Single-Phase Line-Start Permanent-Magnet Synchronous Motor," *IEEE Trans. On Energy Conversion, Vol. 17, No. 4, December 2002.*

[8] Ji-Yong Lee, Sang-Ho Lee, Geun-Ho Lee, Jung-Pyo Hong, Jin Hur, "Determination of Parameters Considering Magnetic Nonlinearity in an Interior Permanent Magnet Synchronous Motor," *IEEE Transaction on Magnetics,* vol. 402, no. 4, April 2006.

[9] Liang Fang, Jae-woo Jung, Jung-Pyo Hong, and Jung-Ho Lee, "Study on High-Efficiency Performance in Interior Permanent-Magnet Synchronous Motor With Double-Layer PM Design," *IEEE Trans. Magn., vol.44, no.11, November 2008*

[10] L. Qinghua, M. A. Jabbar, and M. Khambadkone, "Response surface methodology based design optimization of interior permanent magnet synchronous motors for wide-speed operation," in *Proc. PEMD*, vol. 2, pp. 546-551, March/April 2004.